Homework III in EL2450 Hybrid and Embedded Control Systems

Nadine Drollinger
890120-5420
nadined@kth.se

Alexandros Filotheou
871108-5590
alefil@kth.se

Roberto Sánchez-Rey
840616-9139
rosr@kth.se

Emma Thilén
930715-5466
ethilen@kth.se

Task 22

Figure 1 plots the trajectory of the robot for an experiment performed at KTH's Smart Mobility Lab of the Automatic Control Department. The robot was initially placed in the vicinity of node 2. Its first goal was dictated to be node 1, and from there, nodes 5 and 3.

The robot's bearing and distance tolarance from a target was set to $\xi = 4^\circ$ and the distance tolerance to $\delta = 6$ cm. The controller's gains were set to

$$(\frac{K_\Psi^R}{K_{\Psi,max}^R}, \frac{K_\omega^T}{K_{\omega,max}^T}, \frac{K_\omega^R}{K_{\omega,max}^R}, \frac{K_\Psi^T}{K_{\Psi,max}^T}) \equiv (0.2, 0.2, 0.5, 0.5)$$

where $K_{*,max} > 0$.

The robot's distance errors from nodes 1, 5 and 3 were $e_1 = 8.94$ cm, $e_5 = 6.40$ cm and $e_1 = 6.32$ cm and respectively.

It wasn't before this experiment that we considered a positive K_ω^T, instead of a negative one, as the theoretical analysis pointed to. The second component of the line-following controller showed significantly worse performance when $K_\omega^T < 0$ than when $K_\omega^T > 0$.

When the robot was asked to go from node 2 to node 1, the angle between it and node 1 was $1.68^\circ < \xi = 4^\circ$. Hence, the robot first executed line-following, and not rotation. The augmented error in distance, relative to the other two, is hence the fact that $K_\omega^T < 0$ during the experimental phase.

Figure 2 illustrates the evolution of the position of the robot over time.

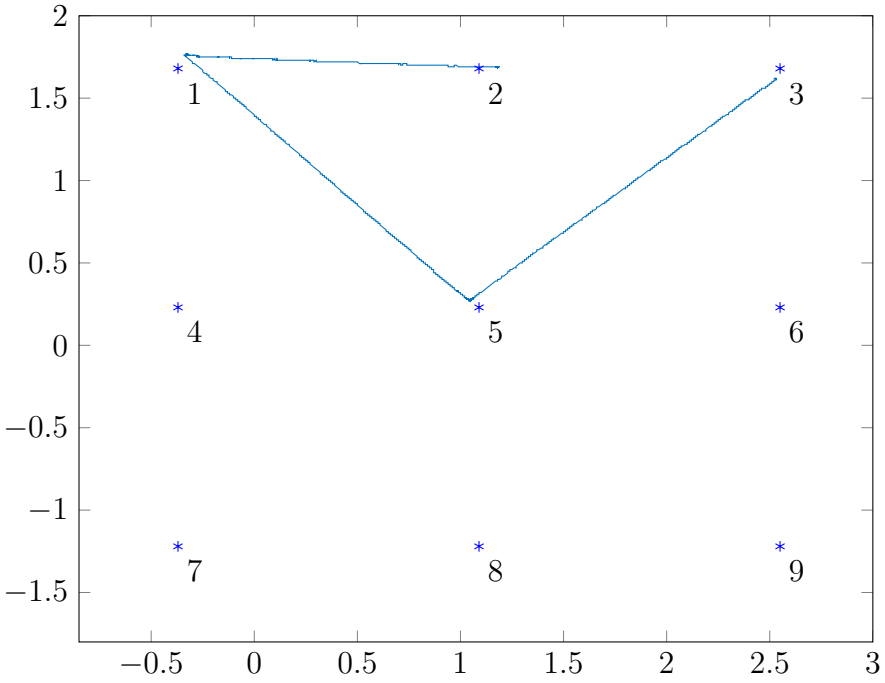

Figure 1: The trajectory of the robot in real-life conditions. The anglular tolerance was set to $\xi = 4°$ and the distance tolerance to $\delta = 6$ cm. Direction of travel is counter-clockwise, starting from node 2.

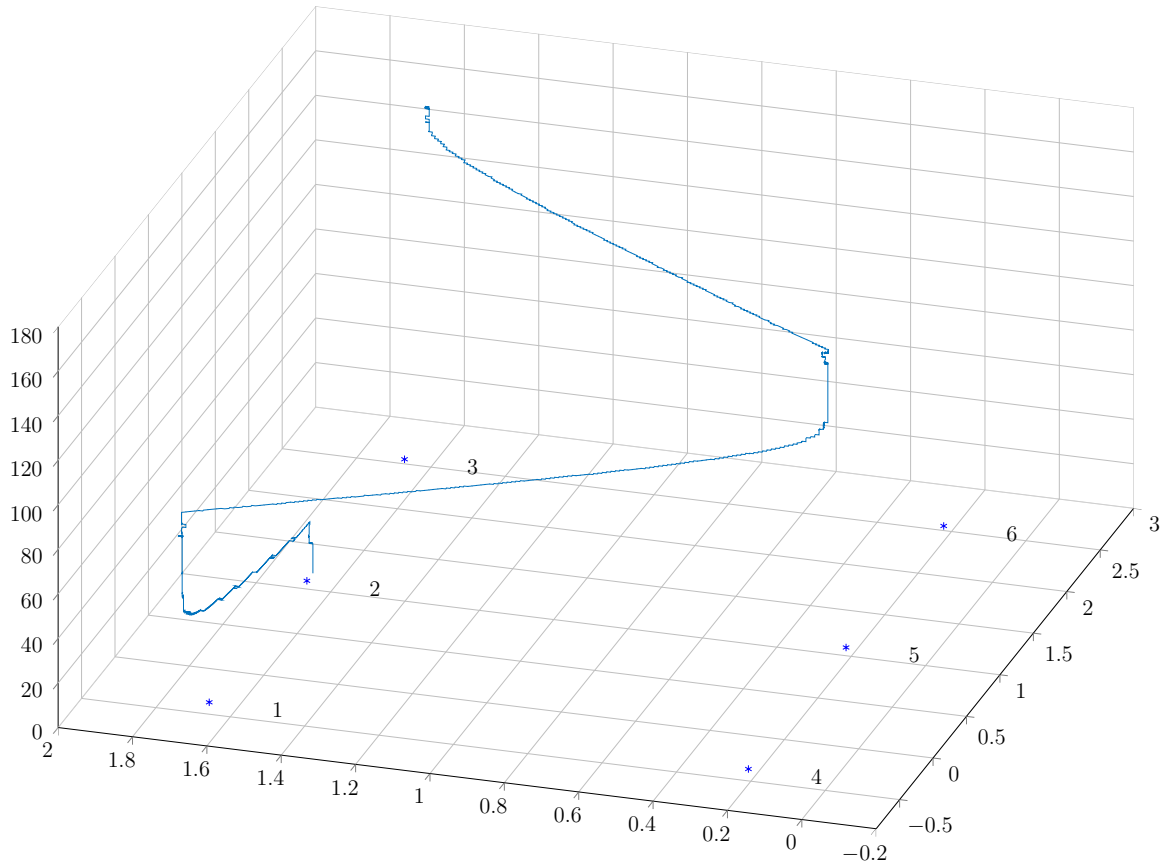

Figure 2: The evolution of the robot's position over time. The vertical axis denotes time units in seconds.

Figure 3 plots the the distance of the robot from the origin $O(0, 0)$ over time for the duration of this experiment. Figures 4, 5, and 6 illustrate the evolution of the error in the robot's distance to each of its three goals.

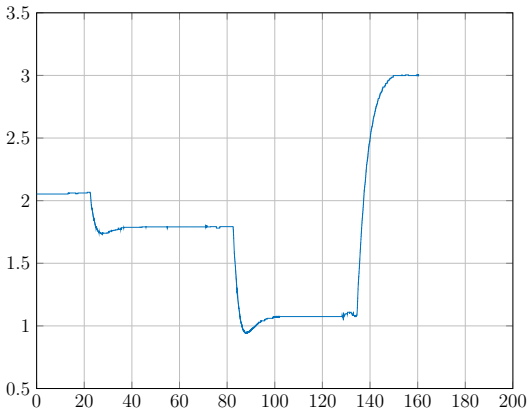

Figure 3: The robot's distance to the origin over time.

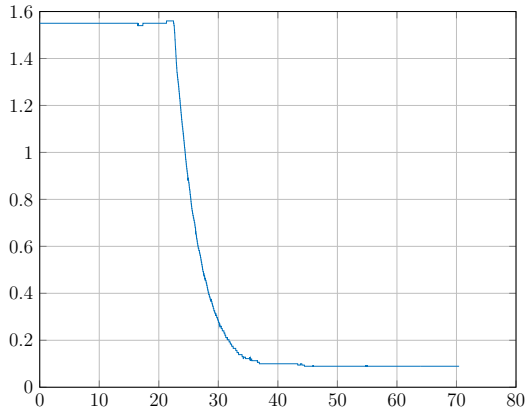

Figure 4: The robot travels from node 2 to node 1. Its steady-state distance error is 8.94 cm.

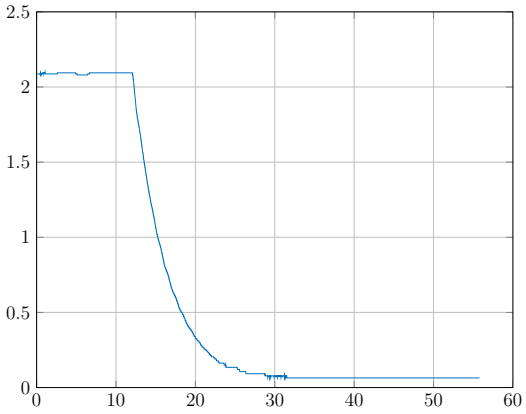

Figure 5: The robot travels from node 1 to node 5. Its steady-state distance error is 6.40 cm.

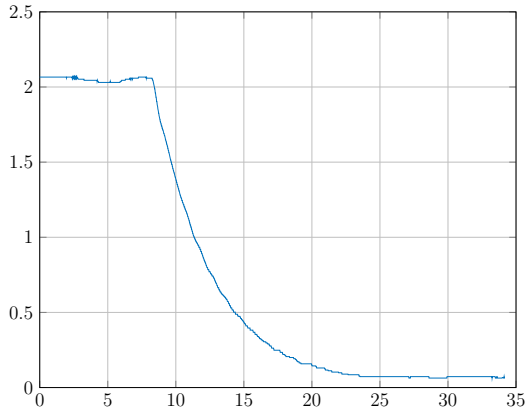

Figure 6: The robot travels from node 5 to node 3. Its steady-state distance error is 6.32 cm.

Figure 7 plots the bearing of the robot over time for the duration of this experiment. Figures 8, 9, and 10 illustrate the evolution of the error in the robot's orientation towards a goal.

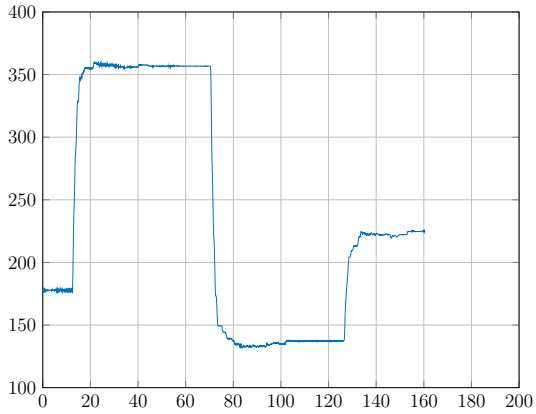

Figure 7: The robot's bearing over the duration of the experiment.

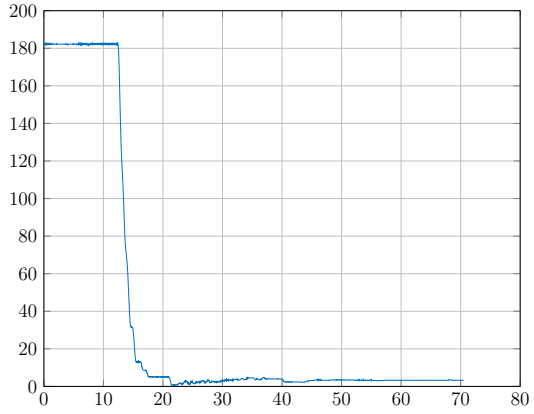

Figure 8: The robot travels from node 2 to node 1. Its steady-state bearing error towards its goal orientation is 3.43°.

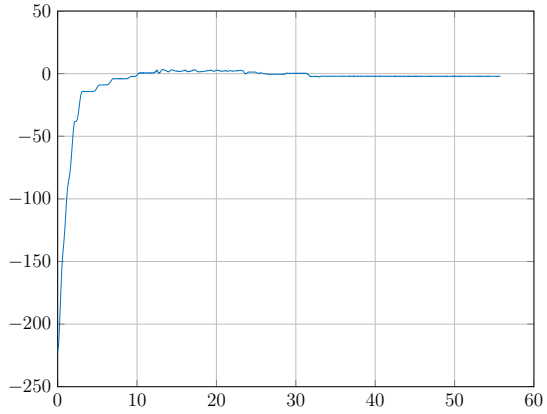

Figure 9: The robot travels from node 1 to node 5. Its steady-state bearing error towards its goal orientation is 2.14°.

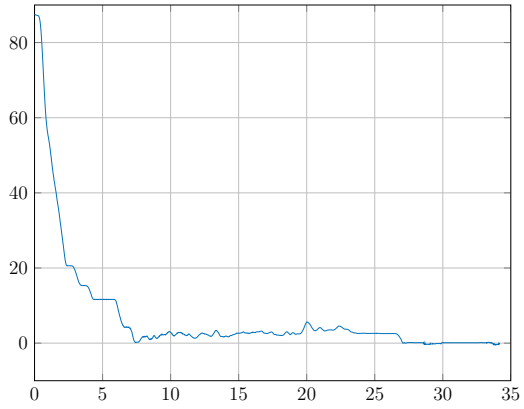

Figure 10: The robot travels from node 5 to node 3. Its steady-state bearing error towards its goal orientation is 0.017°.